

# Squeezing at 946nm with periodically-poled $\text{KTiOPO}_4$

Takao Aoki, Go Takahashi, and Akira Furusawa

Department of Applied Physics, School of Engineering, The University of Tokyo, 7-3-1 Hongo, Bunkyo-ku, Tokyo 113-8656, Japan and CREST, Japan Science and Technology (JST) Agency, 1-9-9 Yaesu, Chuo-ku, Tokyo 103-0028, Japan

Compiled July 3, 2018

We report generation of squeezed vacuum in sideband modes of continuous-wave light at 946nm using a periodically poled  $\text{KTiOPO}_4$  crystal in an optical parametric oscillator. At the pump power of 250mW, we observe the squeezing level of  $-5.6 \pm 0.1\text{dB}$  and the anti-squeezing level of  $+12.7 \pm 0.1\text{dB}$ . The pump power dependence of the observed squeezing/anti-squeezing levels agrees with the theoretically calculated values when the phase fluctuation of locking is taken into account. © 2018 Optical Society of America

OCIS codes: 270.6570, 190.4970.

Suppressed quantum noise of squeezed light can improve the sensitivity of optical measurements that is otherwise limited by the shotnoise.<sup>1,2</sup> In addition to such application to precision measurements, squeezing gives rise to the altered interaction of atoms and light.<sup>3-5</sup> Another application of squeezed light is in the field of continuous-variable quantum information science. Squeezed states are utilized to generate continuous-variable entanglement or to perform quantum nondemolition measurements.<sup>6</sup>

Parametric down conversion processes in subthreshold optical parametric oscillators (OPOs) is often employed to generate continuous-wave squeezed light. Squeezing over  $-6\text{dB}$  has been observed by operating OPOs with nonlinear crystals in non-critical phase matching condition (e.g.  $\text{KNbO}_3$ ,<sup>7</sup>  $\text{LiNbO}_3$ <sup>8</sup>). Although non-critical phase matching enables efficient nonlinear optical couplings, it is possible only in a limited wavelength region. On the other hand, quasi phase matching in periodically-poled materials<sup>9</sup> allows efficient nonlinear optical couplings in a broad range of wavelength. Therefore, these materials are utilized for wavelength conversion<sup>10</sup> and also for generation of squeezed light.<sup>11-14</sup>

The stability of lasers is essential for stable generation of highly squeezed light. In this regard, Diode-pumped Nd:YAG lasers at 1064nm have excellent stability and they have been widely used for generation of squeezed light.<sup>8,15,16</sup> In these experiments, InGaAs photodiodes are commonly used as light-detecting devices. The quantum efficiency of these devices achievable with current technology is about 95%, which results in a 5% detection loss. In contrast, Si photodiodes with quantum efficiencies over 99% are available in the wavelength region from visible to about 950nm. Hence the use of Nd:YAG laser at 946nm<sup>17</sup> and Si photodiodes will reduce the detection loss in these systems. Here we report generation of squeezed vacuum at 946nm using periodically-poled  $\text{KTiOPO}_4$  (PPKTP).

Figure 1 shows the experimental setup. We use a continuous-wave diode-pumped monolithic Nd:YAG laser at 946nm (Innolight Mephisto QTL) with an output power of 500 mW. The second harmonic of the laser

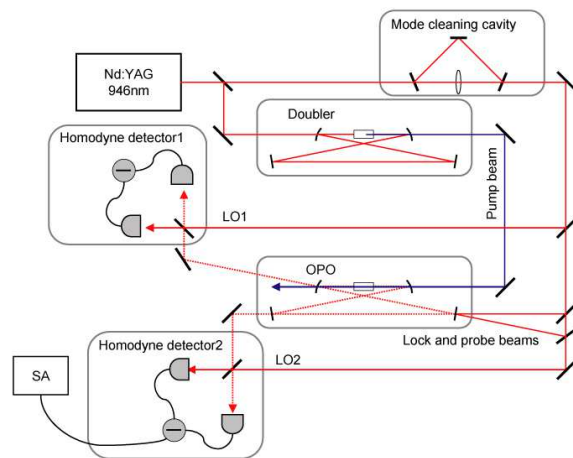


Fig. 1. Experimental setup. LO: local oscillator, OPO: optical parametric oscillator, SA: spectrum analyzer. Homodyne detector1 is used to measure the amplitude of the lock beam to lock the OPO cavity length. AC output of the homodyne detector2 is put into a spectrum analyzer to measure the squeezing/anti-squeezing levels, while DC output is used to lock the LO phase and pump beam phase relative to the probe beam.

is generated in an external-cavity frequency doubler. The frequency doubler has a bow-tie type ring configuration with two spherical mirrors (radius of curvature of 25mm) and two flat mirrors. One of the spherical mirrors has a reflectivity of 90% at 946nm and is used as an input coupler, while the others are high-reflectivity coated. All the mirrors have reflectivities of less than 5% at 473nm. A 10mm-long PPKTP crystal (Raicol Crystals) is used as a nonlinear crystal for second harmonics generation. The cavity length is actively stabilized using the tilt-locking method.<sup>18</sup> The input 946nm beam is slightly misaligned (a few percent in power) in the horizontal direction to have a sufficient error signal. The generated 473nm beam pumps a degenerate optical parametric oscillator (OPO). The OPO also has a bow-tie type ring configuration with two spherical mirrors (radius of curvature of 25mm) and two flat mirrors. One of the flat

mirrors has reflectivity of 85% at 946nm and is used as an output coupler. The round-trip cavity length is 214 mm, which results in a waist radius of  $17\mu\text{m}$  inside the crystal. Again, a 10mm-long PPKTP crystal is used as a nonlinear crystal for parametric down conversion. The OPO is driven below the parametric oscillation threshold to generate squeezed vacuum states. 20mW of 946nm beam from the Nd:YAG laser is spatially filtered in a mode-cleaning cavity with a triangle type ring configuration. The output beam (8mW) is split into four beams: a probe beam, a locking beam, and two local oscillator beams for homodyne detection. The probe beam is injected into the OPO cavity through a high-reflection flat mirror. The transmitted probe beam from the output coupler (100~500nW at parametric gain of 1) is detected with a balanced-homodyne detector. The balanced-homodyne detector has two Si photodiodes (HAMAMATSU S3590-06, anti-reflective coated at 946nm) with quantum efficiency of 99.4% at 946nm. The photocurrents are directly subtracted and put into the AC branch electronics to measure squeezing and the DC branch electronics to lock the local oscillator phase and to measure and lock the parametric gain. The locking beam is also injected into the cavity through a high-reflection flat mirror in the mode counter-propagating to the probe beam. The amplitude of the transmitted beam ( $10\mu\text{W}$ ) is measured with a homodyne detector. The error signal for the dither-locking of the cavity length is extracted from the measured amplitude. The whole setup is on a  $750\text{mm} \times 1200\text{mm}$  breadboard (Newport VH3048W-OPT-28).

Figure 2 shows the measured noise levels at the pump power of 250mW as the local oscillator phase is (i) scanned, (ii) locked at the anti-squeezed quadrature, and (iii) locked at the squeezed quadrature compared to the shotnoise level (iv). The noise level is measured with a spectrum analyzer in the zero span mode at 1MHz, with the resolution bandwidth of 30kHz and the video bandwidth of 300Hz. The traces are averaged for 30 measurements except for (i). The squeezing level of  $-5.6 \pm 0.1\text{dB}$  and the anti-squeezing level of  $+12.7 \pm 0.1\text{dB}$  are observed. By subtracting the detector circuit noise, we obtain the inferred squeezing/anti-squeezing levels of  $-5.80 \pm 0.1\text{dB}$  and  $+12.72 \pm 0.1\text{dB}$ , respectively.

The variance of the output mode  $R_{\pm}$  for the anti-squeezed (+) and the squeezed (-) quadratures can be modeled as<sup>7,19</sup>

$$R_{\pm} = 1 \pm \alpha\rho \frac{4x}{(1 \mp x)^2 + 4\Omega^2}, \quad (1)$$

where  $\alpha$  and  $\rho$  are the detection efficiency and the OPO escape efficiency, respectively. The detection efficiency  $\alpha$  is a product of the propagation efficiency  $\zeta$ , the photodiode quantum efficiency  $\eta$ , and the homodyne efficiency  $\xi^2$  ( $\xi$  is the visibility between the output and the local oscillator modes),  $\alpha = \zeta\eta\xi^2$ . The OPO escape efficiency

can be written as

$$\rho = \frac{T}{T+L}, \quad (2)$$

where  $T$  and  $L$  are the transmission of the output coupler and the intracavity loss, respectively. The pump parameter  $x$  is related to the classical parametric amplification gain  $G$  as

$$G = \frac{1}{(1-x)^2}. \quad (3)$$

The detuning parameter  $\Omega$  is given as the ratio of the measurement frequency  $\omega$  to the OPO cavity decay rate  $\gamma = c(T+L)/l$  ( $l$  = the cavity round trip length),

$$\Omega = \frac{\omega}{\gamma}. \quad (4)$$

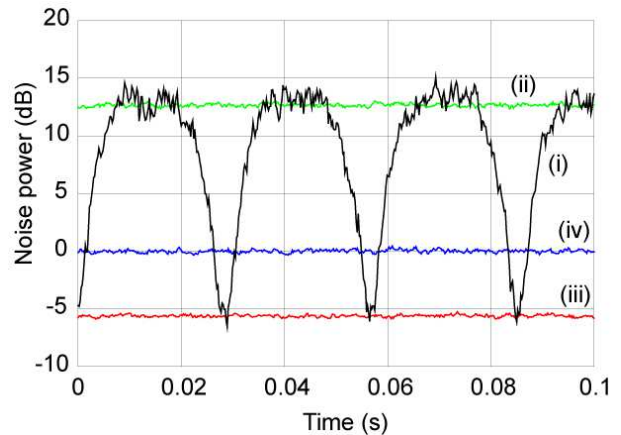


Fig. 2. Measured noise levels at the pump power of 250mW. (i) LO phase is scanned. (ii) LO phase is locked at anti-squeezed quadrature. (iii) LO phase is locked at squeezed quadrature. (iv) Shotnoise level. Noise levels are displayed as the relative power compared to the shotnoise level (0dB). The settings of the spectrum analyzer are, zero-span mode at 1MHz, resolution bandwidth = 30kHz, video bandwidth = 300Hz. All the traces except (i) are averaged for 30 times. Detector circuit noise is not corrected.

In the current setup,  $\zeta \approx 1$ ,  $\eta = 0.994$ ,  $\xi = 0.979$ , therefore  $\alpha = 0.953$ .  $T = 0.15$  and  $L = 0.011$  yield  $\rho = 0.932$ . It should be noted that KTP and PPKTP crystals often suffer from the absorption induced by the pump light<sup>20</sup> as is the case with other nonlinear crystals (e.g.,  $\text{KNbO}_3$ <sup>21</sup>). However, our crystal makes no measurable change of the intracavity loss in the presence of the pump light. We measure the classical parametric amplification gain of  $G = 8.83$ . The detuning parameter is  $\Omega = 0.028$ . With these values, eq. (1) predicts the theoretical squeezing/anti-squeezing levels of  $-8.20\text{dB}$  and  $+13.27\text{dB}$ . Although the theoretical value for the anti-squeezing is consistent with the experiment, there is a discrepancy between them for the squeezing.

This discrepancy may be explained by taking into account the phase fluctuation of the locking.<sup>22</sup> Assuming that the relative phase between the local oscillator and the anti-squeezed/squeezed quadratures has a normal distribution with a small standard deviation of  $\tilde{\theta}$ , the noise levels to be observed can be written as

$$R'_{\pm}(\tilde{\theta}) = \int \frac{1}{\sqrt{2\pi\tilde{\theta}}} \exp\left(-\frac{\theta^2}{2\tilde{\theta}^2}\right) (R_{\pm} \cos^2 \theta + R_{\mp} \sin^2 \theta) d\theta \\ \approx R_{\pm} \cos^2 \tilde{\theta} + R_{\mp} \sin^2 \tilde{\theta}. \quad (5)$$

Therefore, phase fluctuation with an rms of  $\tilde{\theta}$  is effectively equivalent to having a phase offset of  $\tilde{\theta}$ .

From the measurement on the rms noise of the error signal of locking circuits, we obtain the total rms phase fluctuation of  $\tilde{\theta}_{total} = 4.3 \pm 0.6^\circ$ . This results in the corrected theoretical noise levels of  $-5.68 \pm 0.56\text{dB}$  and  $+13.25 \pm 0.1\text{dB}$ , which are in good agreement with the experimentally observed values.

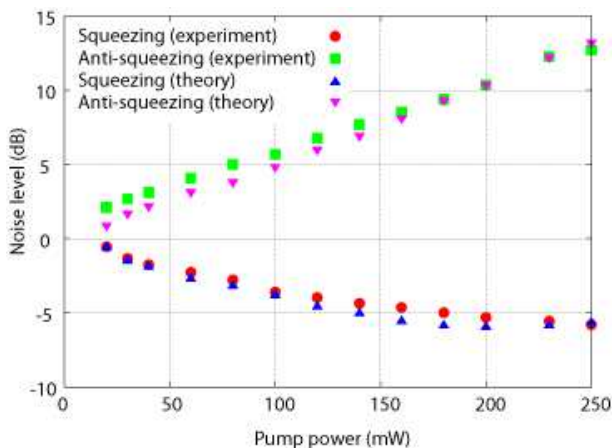


Fig. 3. Pump power dependence of the observed squeezing/anti-squeezing levels (circles/squares) and calculated values (upper/lower triangles) according to eq. (5). Detector circuit noise is corrected for experimentally observed levels.

We repeat the above measurement and analysis for various pump powers. The results are summarized in Fig. 3. Theoretical values fairly agree with the experimental results. The reason for the slight difference in the values of anti-squeezing at low pump powers is not fully understood. Furthermore, we perform the same experiments as Fig. 3 on another PPKTP crystal. We again observe no absorption change induced by the pump light and obtain similar measurement results ( $-5.73 \pm 0.1\text{dB}/+12.22 \pm 0.1\text{dB}$  for squeezing/anti-squeezing levels after correction of the detector circuit noise).

In summary, we observe  $-5.6 \pm 0.1\text{dB}$  squeezing and  $+12.7 \pm 0.1\text{dB}$  anti-squeezing with PPKTP in an OPO. The pump power dependence of the observed squeezing/anti-squeezing levels agree with theoretical model with the phase fluctuation of the locking. Reducing the phase fluctuation by stabilizing the setup

(both actively and passively) may help to observe better squeezing levels.

This work was partly supported by the MPHPT and the MEXT of Japan.

## References

1. E.S. Polzik, J. Carri, and H.J. Kimble, Phys. Rev. Lett **68**, 3020 (1992).
2. C.M. Caves, Phys. Rev. D **23**, 1693 (1981).
3. C.W. Gardiner, Phys. Rev. Lett **56**, 1917 (1986).
4. Q.A. Turchette, N.Ph. Georgiades, C.J. Hood, H.J. Kimble, and A.S. Parkins, Phys. Rev. A **58**, 4056 (1998).
5. P.R. Rice and L.M. Pedrotti, J. Opt. Soc. Am. B **9**, 2008 (1992).
6. S.L. Braunstein and P. van Loock, Rev. Mod. Phys. **77**, 513 (2005).
7. E.S. Polzik, J. Carri, and H.J. Kimble, Appl. Phys. B **55**, 279 (1992).
8. K. Schneider, M. Lang, J. Mlynek, and S. Schiller, Optics Express **2**, 59 (1998).
9. M.M. Fejer, G.A. Magel, D.H. Jundt, and R.L. Byer, IEEE J. Quant. Electron. **28**, 2631 (1992).
10. L.E. Myers, R.C. Eckardt, M.M. Fejer, R.L. Byer, W.R. Bosenberg, and J.W. Pierce, J. Opt. Soc. Am. B **12**, 2102 (1995).
11. M.E. Anderson, M. Beck, M.G. Raymer, and J.D. Bierlein, Opt. Lett. **20**, 620 (1995).
12. D.K. Serkland, M.M. Fejer, R.L. Byer, and Y. Yamamoto, Opt. Lett. **20**, 1649 (1995).
13. D.K. Serkland, P. Kumar, M.A. Arbore, and M.M. Fejer, Opt. Lett. **22**, 1497 (1997).
14. T. Hirano, K. Kotani, T. Ishibashi, S. Okude, and T. Kuwamoto, Opt. Lett. **30**, 1722 (2005).
15. P.K. Lam, T.C. Ralph, B.C. Buchler, D.E. McClelland, H.A. Bachor, and J. Gao, J. Opt. B **1**, 469 (1999).
16. K. McKenzie, N. Grosse, W.P. Bowen, S.E. Whitcomb, M.B. Gray, D.E. McClelland, and P.K. Lam, Phys. Rev. Lett. **93**, 161105 (2004).
17. T.Y. Fan and R.L. Byer, Opt. Lett. **12**, 809 (1987).
18. D.A. Shaddock, M.B. Gray, and D.E. McClelland, Opt. Lett. **24**, 1499 (1999).
19. M.J. Collett and C.W. Gardiner, Phys. Rev. A **30**, 1386 (1984).
20. S. Wang, V. Pasiskevicius, and F. Laurell, J. Appl. Phys. **96**, 2023 (2004).
21. H. Mabuchi, E.S. Polzik, and H.J. Kimble, J. Opt. Soc. Am. B **11**, 2023 (1994).
22. T.C. Zhang, K.W. Goh, C.W. Chou, P. Lodahl, and H.J. Kimble, Phys. Rev. A **67**, 033802 (2003).